

## Reversible and irreversible magnetization of the Chevrel-phase superconductor $\text{PbMo}_6\text{S}_8$

D. N. Zheng, H. D. Ramsbottom, and D. P. Hampshire

*Department of Physics, University of Durham, South Road, Durham DH1 3LE, United Kingdom*

(Received 22 May 1995; revised manuscript received 31 July 1995)

Magnetic measurements have been carried out on the hot-isostatically-pressed Chevrel-phase superconductor  $\text{PbMo}_6\text{S}_8$  at temperatures from 4.2 K to  $T_c$  and for magnetic fields up to 12 T. The results show that for the  $\text{PbMo}_6\text{S}_8$  compound there is a wide magnetically reversible region, between the irreversibility field  $B_{\text{irr}}$  and the upper critical field  $B_{c2}$ , on the isothermal magnetic hysteresis curves. The  $B_{\text{irr}}(T)$  line, i.e., the irreversibility line, was found to obey a power-law expression:  $B_{\text{irr}} = B^*(1 - T/T_c)^\alpha$  with  $\alpha \approx 1.5$ . Magnetic relaxation measurements revealed that the flux-creep effect in the material studied is substantial and is greater than those observed in conventional metallic alloys, but smaller than in high-temperature superconductors. The existence of the irreversibility line and pronounced flux-creep effect in  $\text{PbMo}_6\text{S}_8$  is attributed to the short coherence length of the material. From the reversible magnetization data, the values of the penetration depth, the coherence length, and the critical fields are obtained together with the Ginzburg-Landau parameter  $\kappa$ . At 4.2 K, the critical current density  $J_c$  is  $10^9 \text{ A m}^{-2}$  at zero field, and decreases to  $2 \times 10^8 \text{ A m}^{-2}$  at 10 T. Pinning force curves measured at different temperatures obey a Kramer-scaling law of the form:  $F_p (= J_c \times B) \propto b^{1/2}(1-b)^2$ , which indicates that the  $J_c$  is limited by one predominant flux-pinning mechanism.

### I. INTRODUCTION

One of the important applications of superconductors is to make solenoids that produce very high and yet highly stable magnetic fields. The combination of commercially available materials like NbTi and  $\text{Nb}_3\text{Sn}$  is used to obtain magnetic fields slightly higher than 20 T. Further increases in magnetic field seems unlikely due to the limited upper critical field  $B_{c2}$  of these two materials. Therefore, in order to achieve significantly higher fields, new materials with much higher  $B_{c2}$  have to be explored. Apart from the high-temperature superconducting cuprates, Chevrel-phase superconductors have been regarded as promising candidates for high magnetic-field applications mainly because of their high  $B_{c2}$  values.<sup>1-3</sup> Among Chevrel-phase materials,  $\text{PbMo}_6\text{S}_8$  shows the highest  $B_{c2}$  and the highest superconducting transition temperature  $T_c$ . Thus it has been the subject of much research into its flux pinning and critical current.<sup>4,5</sup>

A critical current density  $J_c$  as high as  $1.5 \times 10^8 \text{ A m}^{-2}$  in 20-T magnetic field has been reported in a  $\text{PbMo}_6\text{S}_8$  wire, and a small coil wound from this wire achieved 84% of short wire  $J_c$ .<sup>6</sup> However, in order to generate magnetic fields higher than 20 T,  $J_c$  values in excess of  $4 \times 10^8 \text{ A m}^{-2}$  are required. The reasons for the comparatively low  $J_c$  values are a subject of the present debate because the mechanisms that control  $J_c$  are still not well understood. Weak links and granularity have been observed and suggested to be responsible for the low  $J_c$ .<sup>6-8</sup> It is now clear that when sintered samples are well-consolidated by hot-isostatic-press processing, the weak links and granularity can be improved or even removed.<sup>6,9</sup> Thus, to increase  $J_c$  of a hot-isostatically-pressed bulk sample significantly it is necessary to increase the density of grain boundaries, which could act as pinning centers as the case in  $\text{Nb}_3\text{Sn}$ , or flux pinning within grains.

Flux pinning and critical currents are closely linked to the microstructure of samples as well as to fundamental super-

conducting properties, such as the coherence length  $\xi$ , the magnetic penetration depth  $\lambda$ , and the critical fields. The very high  $B_{c2}$  of  $\text{PbMo}_6\text{S}_8$  and hence very short coherence length leads to a low pinning energy. Therefore, it is expected that thermal activation plays an important role in the dynamics and stability of the flux-line lattice of  $\text{PbMo}_6\text{S}_8$ .

In this paper, experimental observations of magnetic measurements carried out on hot-isostatically-pressed  $\text{PbMo}_6\text{S}_8$  samples are reported. We show that there is a irreversibility line distinctly below the  $B_{c2}$  line in  $\text{PbMo}_6\text{S}_8$  as seen in high-temperature superconductors. The samples also show a pronounced flux-creep effect. On the other hand, the reversible behavior of the  $\text{PbMo}_6\text{S}_8$  superconductor in the region between the irreversibility line and the  $B_{c2}$  line allows us to measure the equilibrium magnetization and to extract a set of superconducting parameters using Ginzburg-Landau relations. The critical current density is calculated from the magnetic hysteresis using the Bean model<sup>10</sup> from 4.2 K to  $T_c$  and at fields up to 12 T. The pinning force curves measured at different temperatures follow a scaling law. Finally, the effect of the hot-isostatic-pressing temperature on critical currents is discussed.

### II. EXPERIMENTAL

Ceramic  $\text{PbMo}_6\text{S}_8$  samples were prepared by a two-step reaction procedure. Pure elements -Pb (99.9999%), Mo (99.95%, 4-8  $\mu\text{m}$ ) and S (99.999%) were used as starting materials. At first, 10 g of starting materials with nominal compositions  $\text{PbMo}_6\text{S}_8$  were sealed under vacuum in a pre-cleaned silica tube. The tube was then placed in a tube furnace and heat treated at 450 °C for 4 h in an Ar atmosphere. The furnace temperature was then slowly increased to 650 °C at a rate of 33 °C h<sup>-1</sup> and held for 8 h. After this heat treatment, the sample was cooled down quickly to room temperature in about 15 min. The reacted intermediate powder (the mixture of Mo, PbS, and MoS<sub>2</sub>) was ground thor-

oughly using a mortar and pestle and was pressed into discs of 10 mm diameter. The discs were again sealed under vacuum in a precleaned silica tube and reacted at 1000 °C for 44 h in flowing Ar gas to form the  $\text{PbMo}_6\text{S}_8$  phase.

Before performing the hot-isostatic-pressing treatment on the samples, the sintered ceramic samples were ground into powder and repelletized. The pellets were wrapped with Mo foil (99.95%, 0.025 mm thick), which serves as a barrier to prevent the  $\text{PbMo}_6\text{S}_8$  from reacting with the container, and were sealed in a stainless tube under vacuum using hot-spot welding. The hot-isostatic-pressing treatment was carried out at 2000 bars and 800 °C for 8 h. The sample was then extracted from the Mo foil and a rectangular piece,  $5.0 \times 2.8 \times 0.8$  mm, was cut off for magnetic measurements. In addition, three other samples were fabricated and hot-isostatically pressed for 8 h at 1300 bars and at 700, 900, and 1100 °C, respectively.

During the fabrication procedure the  $\text{PbMo}_6\text{S}_8$  samples were handled in a glove box. This ensured that the samples were not exposed to oxygen which degrades the superconducting properties.<sup>11</sup> The glove box maintains a controlled atmosphere such that the oxygen concentration is less than 5 ppm and the moisture level is below 10 ppm. X-ray-diffraction patterns showed that the samples were predominantly single phase. Significant densification after the hot-isostatic-pressing treatment was shown using scanning electron microscopy. The value of  $T_c$  was 13.7 K as measured by ac susceptibility. The transition was sharp ( $\Delta T_c \sim 0.2$  K), indicating that the samples were of good quality.

Magnetic measurements were carried out on a commercial vibrating sample magnetometer (VSM 3001, Oxford Instruments) with the applied field parallel to the longest dimension of the sample. Magnetic hysteresis curves were measured at different temperatures from 4.2 K to  $T_c$ . A 10 min delay was introduced prior to each measurement to ensure temperature stabilization. Magnetic relaxation measurements were performed at 4.2 K and in three different magnetic fields. The field was increased slowly to the required values at  $1 \text{ mT s}^{-1}$  in order to prevent the magnet from overshooting, and the magnetic moment was recorded as a function of time over a period of 10–1800 s.

### III. RESULTS AND DISCUSSION

#### A. Granularity

After the hot-isostatic-press processing, the samples became much more dense and hard than the as-sintered samples, indicating a significant improvement of the connectivity between grains. The density of the samples is estimated to be greater than 90% of the theoretical value. In order to check if granularity is still substantial in the samples, the ratio  $\Delta H/(3\Delta M)$  was measured for the sample fabricated at 2000 bars and 800 °C. Here,  $\Delta H$  is the field range needed to invert the critical state when the applied field is reversed and  $\Delta M$  is the magnetization hysteresis. According to Küpfer *et al.*,<sup>12</sup> the ratio  $\Delta H/(3\Delta M)$  of a rectangular shape sample is unity for a well connected sample, and deviations greater than a factor of 2 indicate granular behavior. The value of  $\Delta H/(3\Delta M)$  at 12 T for the sample used in our study was approximately 1.0, 1.2, 1.1, 1.2, and 0.9 for 4.2, 5, 6, 7, and

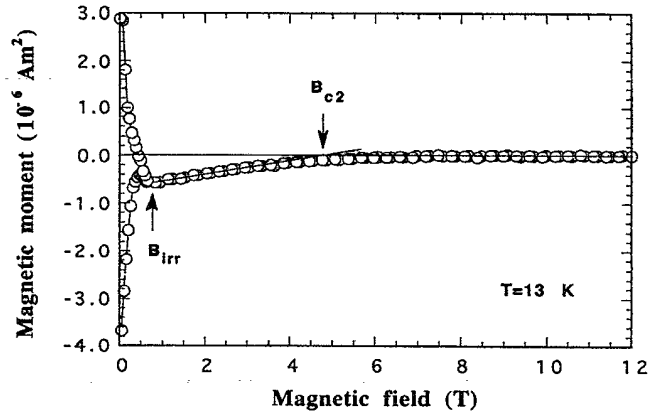


FIG. 1. Magnetic hysteresis loop measured on a  $\text{PbMo}_6\text{S}_8$  sample hot-isostatically pressed at 2000 bars (the background magnetic moment at the normal state had been subtracted). The irreversibility field  $B_{\text{irr}}$  and the upper critical field  $B_{c2}$  were determined as the field at which hysteresis collapses and the field where the moment becomes zero, respectively.

8 K, respectively. This indicates that the irreversible magnetic moment measured is primarily due to macroscopic currents flowing over the full dimensions of a well connected sample. Additional, ac magnetization measurements performed on the same sample, which probe the flux profile inside the sample, support this claim.<sup>13</sup>

#### B. The irreversibility line

The high-temperature superconductors show very strong anisotropy in physical properties due to the two-dimensional nature of their crystal structure. In sharp contrast, the anisotropy of the  $\text{PbMo}_6\text{S}_8$  material is very small. Decroux and Fischer<sup>14</sup> have investigated the anisotropy of several Chevrel-phase superconductors, including  $\text{PbMo}_6\text{S}_8$ , by measuring the angular dependence of  $B_{c2}$  with respect to the symmetry axis of the superconductors. They found that the anisotropy ratio is only 1.2. This anisotropy is negligible compared to the corresponding ratios of high-temperature superconductors. Hence the field-dependent properties of the polycrystalline hot-isostatically-pressed sample should be similar to those of single crystals.

Figure 1 shows the magnetic moment of the  $\text{PbMo}_6\text{S}_8$  sample, fabricated at 2000 bars, measured at 13 K as a function of increasing and decreasing magnetic field. The background contribution, which increases linearly with increasing the field, has been subtracted from the data. The irreversibility field  $B_{\text{irr}}$  is identified as the field at which the magnetic hysteresis  $\Delta M$  collapses. At fields above  $B_{\text{irr}}$ ,  $J_c$  is less than  $10^4 \text{ A m}^{-2}$  (if not zero), and is below the resolution of the instrument. The upper critical field,  $B_{c2}$ , can also be obtained from the data by extrapolating the reversible magnetization to the  $M=0$  line. From  $M$ - $B$  curves measured at different temperatures, the values of  $B_{c2}$  and  $B_{\text{irr}}$  as a function of the temperature are obtained and shown in Fig. 2. This is very similar to the phase diagram determined for high-temperature superconductors.  $B_{\text{irr}}$  data obtained from the Kramer plot extrapolation, as discussed later in Sec. III E, are also shown in the figure represented by the solid symbols.

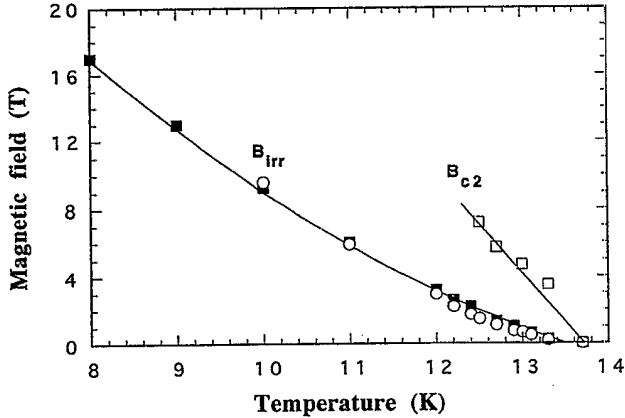


FIG. 2. The irreversibility field  $B_{\text{irr}}$  and the upper critical field  $B_{c2}$  for the  $\text{PbMo}_6\text{S}_8$  sample shown as a function of temperature. Solid square symbols represent  $B_{\text{irr}}$  data obtained from the extrapolation of the Kramer plot (see text). The solid lines are guides for the eye.

In high-temperature superconductors, the existence of the irreversibility line is generally agreed to be a consequence of the very large anisotropy, the short coherence length and high working temperatures of these materials. It was also believed that the reversible flux motion region in low-temperature superconductors would be too small to be easily observed experimentally except for some specially prepared quasi-two-dimensional films such as  $\text{In/InO}$ ,<sup>15</sup> amorphous  $\text{Mo-Ge}$  (Ref. 16) and  $\text{Nb-Ge}$ .<sup>17</sup> Suenaga *et al.*<sup>18</sup> investigated the irreversibility line in conventional  $\text{NbTi}$  and  $\text{Nb}_3\text{Sn}$  materials. They found that the materials have a clear irreversibility line that is substantially lower than the  $B_{c2}$  line. The irreversibility line has also been reported for other low-temperature superconductors.<sup>19,20</sup> For  $\text{PbMo}_6\text{S}_8$  and other Chevrel-phase compounds, there have been several reports on the irreversibility line in the literature.<sup>21-24</sup> The results of Rossel *et al.*<sup>22</sup> measured on a  $\text{PbMo}_6\text{S}_8$  single crystal show a  $B$ - $T$  phase diagram very similar to Fig. 2. However, the size of their magnetic reversible region is significantly larger than we have observed. At 2 T, for instance, we found that the reversible region is about 1.5 K wide (see Fig. 2) while a 4 K difference was reported by Rossel *et al.* The reason for this discrepancy is unclear, but may well be due to the weaker flux pinning of the single crystal in which there could be less chemical or structural imperfections than in hot-isostatically-pressed samples. Furthermore, in terms of the width of the reversible region, the data shown in Fig. 2 appear to agree well with magnetoresistivity data obtained by Gupta *et al.*<sup>25</sup> which show broadened resistive transitions in magnetic fields due to the reversible motion of flux lines. Gupta *et al.* also reported that magnetic-field-induced broadening is more pronounced in  $\text{PbMo}_6\text{S}_8$  than in  $\text{SnMo}_6\text{S}_8$ . This is consistent with the magnetic measurement data for these materials.<sup>24</sup> The difference in broadening between  $\text{PbMo}_6\text{S}_8$  and  $\text{SnMo}_6\text{S}_8$  is possibly because the latter has a longer coherence length (or lower  $B_{c2}$ ) than the former compound.

Figure 3 shows the same data as in Fig. 2 in logarithmic plot of  $B_{\text{irr}}$  versus  $(1 - T/T_c)$ . The linear relation shown in the figure means that the irreversibility line can be described by a power-law expression:

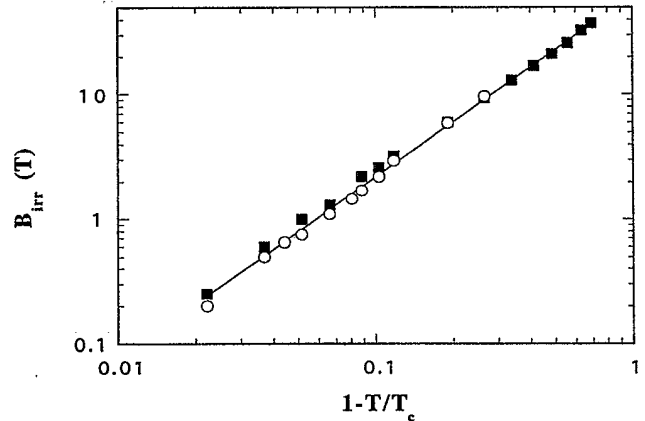


FIG. 3. Logarithmic plot of  $B_{\text{irr}}$  versus  $1 - T/T_c$ . The  $B_{\text{irr}}$  data are the same as those in Fig. 2. The linear behavior of the experimental data indicates a power-law relation  $B_{\text{irr}} \propto (1 - T/T_c)^\alpha$ , and the fitting gives  $\alpha = 1.46$ .

$$B_{\text{irr}} = B^* (1 - T/T_c)^\alpha. \quad (1)$$

A fit to the experimental data yields  $\alpha = 1.46$  and  $B^* = 63$  T. The same relation has been observed on single-crystal samples with slightly different  $\alpha$  and  $B^*$  values.<sup>22</sup> The power-law expression, observed by Müller, Takashige, and Bednorz,<sup>26</sup> has been derived from the thermally activated flux-creep model.<sup>27</sup> It suggests that the irreversibility line is essentially a depinning line.

In order to make a comparison between materials with different fundamental parameters (such as the coherence length) and show the importance of the values of  $\xi$ ,  $B_c$ , and the degree of anisotropy in determining the range of the flux-line reversibility, we present the irreversibility line data for four different superconductors in Fig. 4. For each material, fields and temperatures have been normalized to their own  $B_{c2}(0)$  and  $T_c$  values, respectively. The data are shown for the alloy  $\text{NbTi}$ , the noncuprate oxide  $\text{Ba}(\text{Pb}_{0.75}\text{Bi}_{0.25})\text{O}_3$  and the high-temperature cuprate  $\text{YBa}_2\text{Cu}_3\text{O}_7$  as well as for  $\text{PbMo}_6\text{S}_8$ . The data of the first three materials were obtained

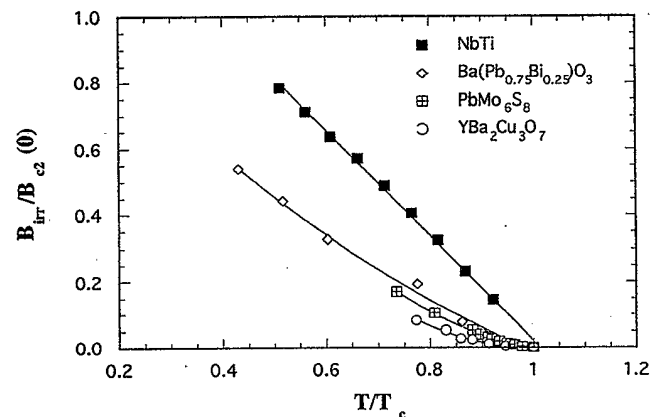


FIG. 4. Normalized plot of the irreversibility line for  $\text{PbMo}_6\text{S}_8$ ,  $\text{NbTi}$ ,  $\text{Ba}(\text{Pb}_{0.75}\text{Bi}_{0.25})\text{O}_3$  and  $\text{YBa}_2\text{Cu}_3\text{O}_7$  ( $B \parallel c$  axis). The solid lines are guides for the eye.

in previous studies.<sup>28–30</sup> It is not surprising to find in the figure that NbTi, which has a comparatively long coherence length and is isotropic, exhibits an irreversibility line that is very close to its  $B_{c2}$  line, while for the high-temperature superconductor YBa<sub>2</sub>Cu<sub>3</sub>O<sub>7</sub> the irreversibility line is strongly depressed because of its high anisotropy and short coherence length. The coherence length of PbMo<sub>6</sub>S<sub>8</sub> (which will be calculated in the following section) lies between that of NbTi and YBa<sub>2</sub>Cu<sub>3</sub>O<sub>7</sub>, and thus we found the irreversibility line of PbMo<sub>6</sub>S<sub>8</sub> is also located in an intermediate position in the phase diagram. For the Ba(Pb<sub>0.75</sub>Bi<sub>0.25</sub>)O<sub>3</sub> compound, the irreversibility line is also strongly depressed although its coherence length is much longer than the other materials shown in the figure. This may result from its low value of thermodynamic critical field  $B_c$ ,<sup>29</sup> which is approximately one order of magnitude less than that of NbTi and PbMo<sub>6</sub>S<sub>8</sub> and thus leads to a small pinning energy (which is proportional to  $B_c^2$ ).

It has been argued that the irreversibility line of NbTi and other low-temperature materials such as Nb<sub>3</sub>Sn and Nb can be better described as flux-lattice melting line.<sup>18–20,31</sup> The data presented here for the PbMo<sub>6</sub>S<sub>8</sub> fit the expression based on the thermally activated depinning model well. Regardless of the mechanism of the magnetic reversible behavior in the low-temperature superconductors, it is safe to say that the short coherence length is a major factor that leads to a very low irreversibility line for PbMo<sub>6</sub>S<sub>8</sub>.

### C. Superconducting parameters

The basic parameters in the superconducting state such as the coherence length  $\xi$ , the magnetic-field penetration depth  $\lambda$ , the Ginzburg-Landau parameter  $\kappa$ , and the various critical fields are of great importance, both for understanding flux-pinning mechanism as well as the superconducting pairing mechanism. The reversible behavior in the region above the irreversibility line permits the equilibrium magnetization to be measured so that the parameters can be extracted.

Using the data shown in Fig. 2, the initial slope of  $B_{c2}$  near  $T_c$  is found to be 5.9 T K<sup>-1</sup>. This value is in agreement with the specific-heat data measured on the same sample<sup>32</sup> and the data reported in the literature.<sup>3,5,33</sup> The value of  $B_{c2}$  extrapolated to zero temperature is 56 T using the relation<sup>34</sup>

$$B_{c2}(0) = 0.7T_c(\partial B_{c2}/\partial T)|_{T_c}. \quad (2)$$

According to the theory of Abrikosov,<sup>35</sup> the linear magnetization near to  $B_{c2}$  is described by

$$-\mu_0 M = (B_{c2} - B)/[\beta_A(2\kappa^2 - 1)]. \quad (3)$$

Hence the value of  $\kappa$  can be obtained from the slope of the magnetization versus field data in the linear region. Using the data collected at 12.7, 13, and 13.3 K, the value at each temperature is calculated and the average value for  $\kappa$  found to be 130. Other superconducting parameters can be calculated by employing the Ginzburg-Landau relations: From  $B_{c2} = \sqrt{2}\kappa B_c$  and  $B_{c1} = B_c(\ln \kappa + 0.5)/(\sqrt{2}\kappa)$ , the initial slope of  $B_c$  and  $B_{c1}$  is found to be  $-32$  mT K<sup>-1</sup> and  $-0.94$  mT K<sup>-1</sup>, respectively. For  $B_c$ , the zero-temperature value is obtained by using the BCS expression:<sup>36</sup>

TABLE I. Zero-temperature values of the superconducting parameters of the PbMo<sub>6</sub>S<sub>8</sub> sample. The values were determined from the reversible magnetization data.

$T_c$ (K)	$\kappa$	$B_{c2}$ (T)	$B_{c1}$ (mT)	$B_c$ (T)	$\lambda$ (nm)	$\xi$ (nm)
13.7	130	56	6.4	0.25	230	2.0

$B_c(T) = 1.74B_c(0)[1 - T/T_c]$  which gives  $B_c(0) = 0.25$  T. Since there is no theoretical expression for the temperature dependence of  $B_{c1}$ , a reasonable approximation to obtain  $B_{c1}(0)$  is to use the empirical relation  $B_{c1}(T) = B_{c1}(0)[1 - (T/T_c)^2]$  which yields  $B_{c1}(0) = 6.4$  mT. Using  $B_{c2}(T) = \Phi_0/[2\pi\xi^2(T)]$  (where  $\Phi_0 = 2.07 \times 10^{-15}$  Wb is the flux quantum),  $\xi(T) = \xi(0)[1 - T/T_c]^{-1/2}$  and  $\kappa = \lambda(0)/\xi(0)$ ,  $\xi(0)$  and  $\lambda(0)$  are calculated to be 2.0 and 230 nm, respectively. The values of all the parameters obtained are shown in Table I. The  $B_c$  value is close to the value (0.27 T) reported by Seeber, Rossel, and Fischer,<sup>37</sup> while the  $\lambda$  value is only slightly larger than the value (200–240 nm) estimated from positive-muon spin-rotation studies.<sup>38</sup> The very large  $\kappa$  value shows that PbMo<sub>6</sub>S<sub>8</sub> is an extreme type-II superconductor. The short coherence length leads to easy thermal activation of flux lines as discussed in the previous (and the following) section, and also makes this compound sensitive to disorder and local defects.

### D. Magnetic relaxation

Magnetic relaxation curves measured at 4.2 K and for 1, 6, and 12 T are shown in Fig. 5. The irreversible magnetic moment is expected to decay with time as flux lines creep into the specimen. In all the data shown here, the equilibrium magnetic moment  $m_{eq}$  [ $\approx (m_+ + m_-)/2$ ], which was approximated by the average of the magnetic moment for increasing ( $m_+$ ) and decreasing ( $m_-$ ) field,<sup>39</sup> has been subtracted. The data are also normalized to the magnetic moment value at  $t = 10$  s for the three curves. As expected by the theory,<sup>40</sup> the moment appears to decay linearly with

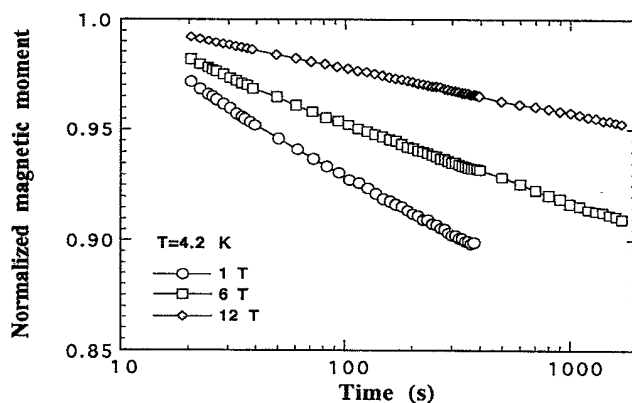


FIG. 5. Magnetic relaxation data taken at 4.2 K and three different fields. The equilibrium magnetic moment data  $m_{eq}$  ( $\approx [m_+ + m_-]/2$ ), which was approximated as the average of the magnetic moment for increasing ( $m_+$ ) and decreasing ( $m_-$ ) field, has been subtracted from the data. The data are normalized to the value at  $t = 10$  s.

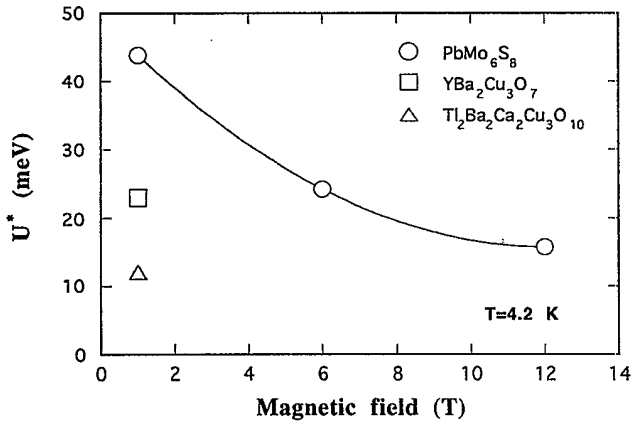


FIG. 6. Apparent pinning energy  $U^*$  calculated from the flux-creep data using a simple Anderson-Kim model  $m = m(0)[1 - (k_B T/U^*) \ln(t)]$  for the  $\text{PbMo}_6\text{S}_8$  sample. Data of  $\text{YBa}_2\text{Cu}_3\text{O}_7$  and  $\text{Tl}_2\text{Ba}_2\text{Ca}_2\text{Cu}_3\text{O}_{10}$  measured at 1 T are also shown. The solid line is a guide for the eye.

$\ln(t)$  for all three fields. An apparent pinning energy  $U^*$  can be obtained on the basis of this observation by using the formula<sup>40</sup>

$$m(t) = m(0)[1 - (k_B T/U^*) \ln(t)]. \quad (4)$$

Although  $U^*$  may not represent the true depth of the pinning well,<sup>41</sup> a comparison of the results obtained under similar experimental conditions is still meaningful.

A plot of  $U^*$  as a function of the applied field is shown in Fig. 6. Data of  $\text{YBa}_2\text{Cu}_3\text{O}_7$  and another high-temperature cuprate  $\text{Tl}_2\text{Ba}_2\text{Ca}_2\text{Cu}_3\text{O}_{10}$  measured at 1 T are also shown in the figure for a comparison. We have attempted to measure magnetic relaxations for a NbTi sample at 1 T. However, no decay in the magnetic moment was observed within the resolution of the instrument used. Thus we may conclude that the flux-creep effect in  $\text{PbMo}_6\text{S}_8$  is more pronounced than in NbTi yet smaller than  $\text{YBa}_2\text{Cu}_3\text{O}_7$  and other high-temperature superconductors. This is consistent with the irreversibility line results discussed in the previous section and can be understood by considering the value of the coherence length and anisotropy of these materials.

### E. Critical current density and pinning force

Magnetic hysteresis curves have been measured at temperatures from 4.2 K to  $T_c$  and for fields up to 12 T. The critical current density  $J_c$  is calculated from the magnetic hysteresis data using the Bean model.<sup>10</sup> For the rectangular samples used in our measurements,

$$J_c (\text{A m}^{-2}) = \Delta M / [a_2(1 - a_2/3a_1)] \quad (5)$$

where  $\Delta M$  ( $\text{A m}^{-1}$ ) is the difference in magnetization for increasing and decreasing field, and  $2a_1$  (m) and  $2a_2$  (m) ( $a_1 > a_2$ ) is the width and thickness of samples, respectively. The magnetic-field dependence of  $J_c$  for different temperatures is shown in Fig. 7. For temperatures 5, 6, and 7 K, measurements were started at about 1 T. The  $J_c$  of the sample fabricated at 2000 bars and 800 °C at 4.2 K is slightly higher than  $10^9 \text{ A m}^{-2}$  at zero field and decreases to

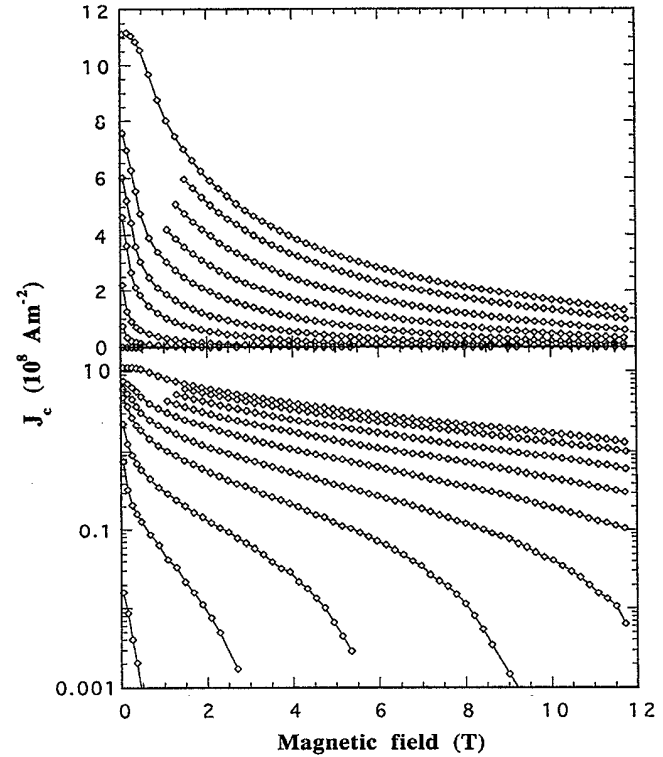


FIG. 7. (Top): Critical current density  $J_c$  of the  $\text{PbMo}_6\text{S}_8$  sample as a function of applied magnetic field and temperature. (Bottom): Semilogarithmic plot of  $J_c$  versus  $B$  for the same data.  $J_c$  values were calculated from magnetic hysteresis data using the Bean model. From top to bottom: 4.2, 5, 6, 7, 8, 9, 10, 11, 12, and 13 K.

$2 \times 10^8 \text{ A m}^{-2}$  at 10 T. The  $J_c$  values are in the same general range as the reported critical current densities measured on hot-isostatically-pressed wires and bulk samples.<sup>6,9,42,43</sup>

There have been reports of flux jumps in the magnetic hysteresis curves of  $\text{PbMo}_6\text{S}_8$  samples measured at temperatures far below  $T_c$ .<sup>24,44,45</sup> These type of jumps have also been reported for other highly irreversible superconductors and are due to the low thermal conductivity of these materials. However, measurements on the hot-isostatically-pressed  $\text{PbMo}_6\text{S}_8$  samples used in this study show no sign of flux jumps. The absence of the flux jumps is possibly due to the slow magnetic-field sweeping rate ( $20 \text{ mT s}^{-1}$ ) used, or the thermal environment of the experiment.

Figure 8 shows a normalized plot of pinning force density  $F_p (= J_c \times B)$  as a function of the applied field for temperatures from 4.2 to 13 K derived from the data in Fig. 7. At each temperature the  $F_p$  values are normalized to the maximum  $F_p$  value  $F_{p\text{max}}$  and the fields are normalized to the irreversibility field  $B_{\text{irr}}$  at this temperature (low-temperature  $B_{\text{irr}}$  values were obtained by extrapolation as will be shown later in Fig. 9). As shown in Fig. 8,  $F_p$  curves measured at different temperatures obey a universal scaling law.<sup>46</sup> Strictly speaking, curves measured at low temperatures (below 10 K where  $J_c$  does not reach zero at the highest available field 12 T) are not complete and it is not clear if the scaling behavior operates at very low temperatures. However, based on the

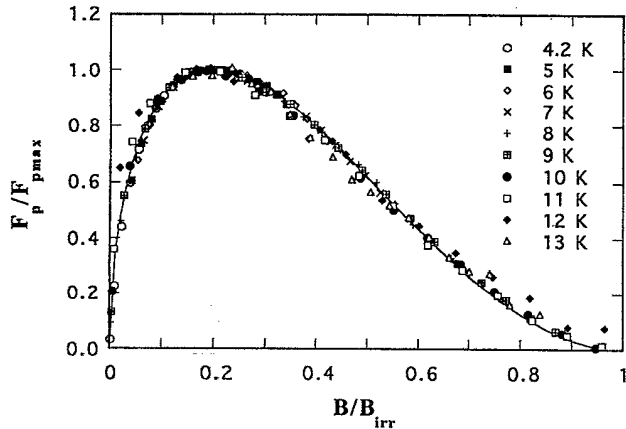


FIG. 8. Normalized pinning force as a function of normalized magnetic field for the  $\text{PbMo}_6\text{S}_8$  sample. The solid line represents the normalized function proportional to  $b^{1/2}(1-b)^2$ .

data shown in Fig. 9, it is not unreasonable to assume that the scaling will continue at low temperatures.

The scaling of the pinning force in type-II superconductors, reported by Fietz and Webb,<sup>46</sup> has generated a great deal of theoretical work in order to calculate the elementary pinning force on each individual flux line and to propose a summation procedure to obtain the total pinning force.<sup>47</sup> Although the summation problem has not yet been solved satisfactorily, most of observed magnetic-field dependence of  $F_p$  can be expressed by the scaling law,<sup>46</sup>

$$F_p = \gamma B_{c2}^n(T) b^p (1-b)^q, \quad (6)$$

where  $b$  is the reduced field  $B/B_{c2}$ , and  $n$ ,  $p$ , and  $q$  are constants depending on the nature and density of the pinning centres. The quantity  $\gamma$  is a constant dependant on the microstructure and the Ginzburg-Landau parameter. Usually if only one pinning mechanism operates at all temperatures and fields, the pinning force scales according to the equation above. Thus, the scaling curve shown in Fig. 8 indicates that the  $J_c$  in our sample is mainly limited by one mechanism. Furthermore, the scaling curve in Fig. 8 can be described by

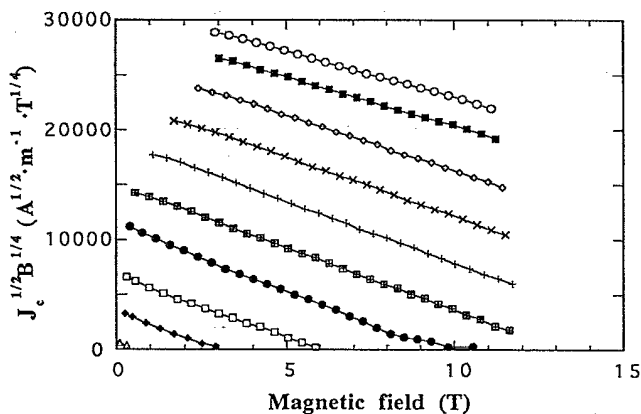


FIG. 9. A Kramer plot ( $J_c^{1/2} B^{1/4}$  versus  $B$ ) for the  $\text{PbMo}_6\text{S}_8$  sample. From top to bottom: 4.2, 5, 6, 7, 8, 9, 10, 11, 12, and 13 K.

the expression derived by Kramer<sup>48</sup> for the flux-lattice shearing mechanism, and later by Dew-Hughes,<sup>49</sup> Hampshire and Jones<sup>50</sup> from different approaches, which gives  $p=1/2$  and  $q=2$  in Eq. (6), i.e.,

$$F_p = J_c \times B = \gamma B_{\text{irr}}^{5/2}(T) b^{1/2} (1-b)^2. \quad (7)$$

This is clearly illustrated in Fig. 9 in which  $J_c^{1/2} B^{1/4}$  is plotted against the applied field. The linear behavior shown in the figure demonstrates the validity of Eq. (7). The exponent 5/2 is valid in so far as the gradient of the lines in the Kramer plots (Fig. 9) are independent of temperature. The linear extrapolation of the data for each temperature to the  $J_c^{1/2} B^{1/4}=0$  line gives  $B_{\text{irr}}$  values at corresponding temperatures. At temperatures close to  $T_c$ , the values of  $B_{\text{irr}}$  derived from the Kramer plots are in agreement with those determined from the magnetic hysteresis loops in Fig. 1. The similarity between the field at which  $J_c$  drops to zero and the characteristic field in the scaling law suggests that the mechanism that causes the irreversibility line plays an integral role in determining  $J_c$  throughout the irreversible region of the  $B$ - $T$  phase diagram. The form of the scaling law is similar to that commonly observed in  $\text{Nb}_3\text{Sn}$  (where grain boundaries are major pinning centres), and has led Rickel, Togonidze, and Tsebro<sup>51</sup> and Bonney, Willis, and Larbalestier<sup>24,25</sup> to propose a grain-boundary pinning mechanism in  $\text{PbMo}_6\text{S}_8$ .

Using a model assuming an optimal arrangement of pinning centers where all flux lines are pinned,<sup>52</sup> Rossel *et al.* have estimated the maximum possible critical current density for  $\text{PbMo}_6\text{S}_8$ . They found it should be above  $10^{10} \text{ A m}^{-2}$  at 4.2 K and 20 T, one order of magnitude higher than the best experimental results. It has been suggested that using low fabrication temperature to reduce grain size and increase grain-boundary pinning centers will improve  $J_c$ .<sup>24,45</sup> In  $\text{Nb}_3\text{Sn}$ , high  $J_c$  has been achieved by reducing the size of grains. Experimental results suggest this is a plausible way.<sup>24,44,45</sup> However, it is not clear if  $J_c$  can be increased by as much as it has been achieved in  $\text{Nb}_3\text{Sn}$  by merely reducing grain size. Karasik *et al.*<sup>53</sup> have shown that the maximum value of the pinning force saturated when the grain size is less than  $0.3 \mu\text{m}$ . Alternatively, Rossel and Fischer<sup>44</sup> have shown that artificially introducing pinning centers by neutron irradiation and the addition of fine nonsuperconducting particles in hot-pressed samples can increase  $J_c$  of  $\text{PbMo}_6\text{S}_8$  samples.

Several ceramic samples made under identical conditions have been hot-isostatically pressed at 1300 bars and 700, 900, and 1100 °C, respectively. Figure 10 shows the  $J_c$  of these three samples measured at 4.2 K. In Fig. 11,  $J_c$  measured at 3 T and two temperatures is plotted against the hot-isostatic-pressing temperature. It is interesting to note that  $J_c$  varies nonmonotonically with the temperature. Although 900 °C seems to be an optimum temperature for maximizing  $J_c$ , one should be cautious before generalizing the result in Fig. 11 since  $J_c$  is controlled by many factors. Nevertheless, for Fig. 11, it is possible to give a qualitative explanation. When samples are hot-isostatically pressed at low temperatures, incomplete sintering at grain boundaries may result if the reaction time is not long enough, leading to lower  $J_c$  values. Alternatively, at high temperatures, the superconduct-

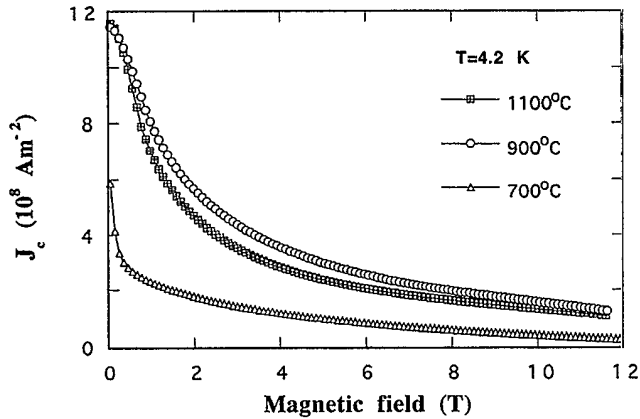


FIG. 10. Critical current density  $J_c$  measured at 4.2 K for three  $\text{PbMo}_6\text{S}_8$  samples hot-isostatically pressed at three different temperatures and 1300 bars.

ing properties at the grain boundaries may degrade due to the loss of one or more elements. The degraded grain boundaries reduce the  $J_c$  of bulk materials. A similar relation between  $J_c$  and fabrication temperature has also been reported on uniaxially hot-pressed  $\text{SnMo}_6\text{S}_8$  samples by Gupta *et al.*<sup>54</sup>

#### IV. SUMMARY

In summary, systematic magnetization measurements have been performed on the hot-isostatically-pressed Chevrel-phase superconductor  $\text{PbMo}_6\text{S}_8$ . An irreversibility line  $B_{\text{irr}}(T)$ , which is considerably lower than the superconducting phase transition line  $B_{c2}(T)$ , is identified for the  $\text{PbMo}_6\text{S}_8$  material. The temperature dependence of  $B_{\text{irr}}$  was found to follow a power-law relation:  $B_{\text{irr}}(T) \propto (1 - T/T_c)^\alpha$  with  $\alpha \approx 1.5$ . Magnetic relaxation measurements show that the flux-creep effect in  $\text{PbMo}_6\text{S}_8$  materials is larger than metallic NbTi alloy but smaller than high- $T_c$  materials. The existence of the wide magnetic reversible region and the pronounced flux-creep effect is attributed to the short coherence length of the material. A set of superconducting parameters, including the coherence length  $\xi$ , the penetration depth  $\lambda$ , the critical fields and the Ginzburg-Landau parameter  $\kappa$  have

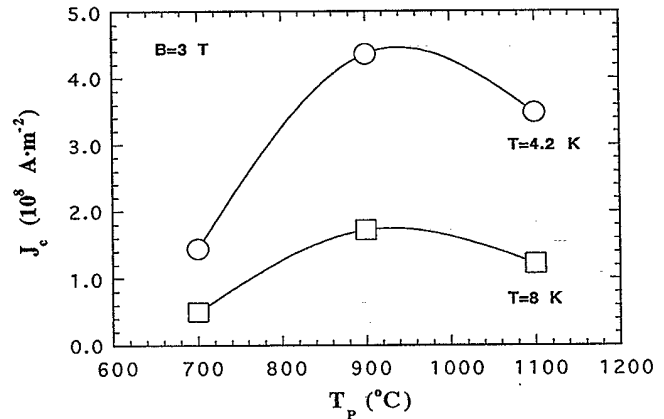


FIG. 11. Critical current density (at 3 T and 4.2, 8 K) versus the hot-isostatic pressing temperature.

been evaluated using reversible magnetization data for  $\text{PbMo}_6\text{S}_8$ . For the sample fabricated at 2000 bars and 800 °C,  $J_c$  at 4.2 K is  $10^9 \text{ A m}^{-2}$  at zero field which decreases to  $2 \times 10^8 \text{ A m}^{-2}$  at 10 T. Reduced pinning force curves measured at temperatures from 4.2 K to  $T_c$  appear to follow the Kramer scaling law, indicating that the  $J_c$  is limited by one predominant flux-pinning mechanism.  $J_c$  data measured on the samples hot-isostatically pressed at different temperatures show a nonmonotonic relation between  $J_c$  and the processing temperature.

#### ACKNOWLEDGMENTS

The authors would like to thank A. Crum (Engineered Pressure Systems/National Forge Europe) for the use of the hot-isostatic-press system, D. Astill, and W. Y. Liang (University of Cambridge) for the use of the vibrating sample magnetometer. Invaluable discussions with L. Le Lay (BICC Superconductors, UK), N.J.C. Ingle and T. C. Wills (University of Wisconsin-Madison), and A.M. Campbell (University of Cambridge) are greatly appreciated. This work was supported by the Engineering and Physical Sciences Research Council UK and the Royal Society.

<sup>1</sup>Ø. Fischer, R. Odermatt, G. Bongi, H. Jones, R. Chevrel, and M. Sergent, *Phys. Lett.* **45A**, 87 (1973).

<sup>2</sup>R. Odermatt, Ø. Fisher, H. Jones, and G. Bongi, *J. Phys. C* **7**, L13 (1974).

<sup>3</sup>S. Foner, E. J. McNiff, Jr., and E. J. Alexander, *Phys. Lett.* **49A**, 269 (1974).

<sup>4</sup>B. Seeber, M. Decroux, and Ø. Fischer, *Physical B* **155**, 129 (1989).

<sup>5</sup>M. Decroux, P. Selvam, J. Cors, B. Seeber, and Ø. Fischer, *IEEE Trans. Appl. Supercond.* **3**, 1502 (1993).

<sup>6</sup>H. Yamasaki, M. Umeda, S. Kosaka, Y. Kimura, T. C. Willis, and D. C. Larbalestier, *J. Appl. Phys.* **70**, 1606 (1991).

<sup>7</sup>M. Decroux, D. Cattani, J. Cors, S. Ritter, and Ø. Fischer, *Physica B* **165-166**, 1395 (1990).

<sup>8</sup>D. Cattani, J. Cors, M. Decroux, and Ø. Fischer, *IEEE Trans. Mag.* **27**, 950 (1991).

<sup>9</sup>L. Le Lay, T. C. Willis, and D. C. Larbalestier, *Appl. Phys. Lett.* **60**, 775 (1992).

<sup>10</sup>C. P. Bean, *Rev. Mod. Phys.* **36**, 31 (1964).

<sup>11</sup>S. Foner, E. J. McNiff, Jr., and D. G. Hinks, *Phys. Rev. B* **31**, 6108 (1985).

<sup>12</sup>H. Küpfer, C. Keller, A. Gurevich, K. Salama, and V. Selvamanickam, in *Advances in Superconductivity III*, edited by K. Kajimura and H. Hayakawa (Springer-Verlag, 1991), p. 709.

<sup>13</sup>H. D. Ramsbottom, D. N. Zheng, and D. P. Hampshire, *IEEE Trans. Appl. Supercond.* **5**, 1321 (1995).

<sup>14</sup>M. Decroux and Ø. Fischer, in *Superconductivity in Ternary Compounds*, edited by Ø. Fischer and M. B. Maple, *Topics in Cur-*

- rent *Physics Vol. 34* (Springer, Berlin, 1982), Vol. 2, p. 57.
- <sup>15</sup>P. L. Gammel, A. F. Hebard, and D. J. Bishop, *Phys. Rev. Lett.* **60**, 144 (1988).
  - <sup>16</sup>J. M. Graybeal and M. R. Beasley, *Phys. Rev. Lett.* **56**, 173 (1986).
  - <sup>17</sup>P. Berghuis, A. L. F. van der Slot, and P. H. Kes, *Phys. Rev. Lett.* **65**, 2583 (1990).
  - <sup>18</sup>M. Suenaga, A. K. Ghosh, Y. Xu, and D. O. Welch, *Phys. Rev. Lett.* **66**, 1777 (1991).
  - <sup>19</sup>M. F. Schmidt, N. E. Israeloff, and A. M. Goldman, *Phys. Rev. B* **48**, 3404 (1993).
  - <sup>20</sup>H. Drulis, Z. G. Xu, J. W. Brill, L. E. De Long, and J.-C. Hou, *Phys. Rev. B* **44**, 4731 (1991).
  - <sup>21</sup>M. Suenga, D. O. Welch, and R. Budhani, *Supercond. Sci. Technol.* **5**, S1 (1992).
  - <sup>22</sup>C. Rossel, O. Peña, H. Schmitt, and M. Sergent, *Physica C* **181**, 363 (1991).
  - <sup>23</sup>C. Rossel, E. Sandvold, M. Sergent, R. Chevrel, and M. Potel, *Physica C* **165**, 223 (1990).
  - <sup>24</sup>L. A. Bonney, T. C. Willis, and D. C. Larbalestier, *J. Appl. Phys.* **77**, 6377 (1995).
  - <sup>25</sup>A. Gupta, M. Decroux, T. C. Willis, and Ø. Fischer, *Physica C* **235**, 2541 (1994).
  - <sup>26</sup>K. A. Müller, M. Takashige, and J. G. Bednorz, *Phys. Rev. Lett.* **58**, 1143 (1987).
  - <sup>27</sup>Y. Yeshurun and A. P. Malozemoff, *Phys. Rev. Lett.* **60**, 2202 (1988).
  - <sup>28</sup>D. N. Zheng, N. J. C. Ingle, and A. M. Campbell (unpublished).
  - <sup>29</sup>D. N. Zheng, Ph.D. thesis, University of Cambridge, 1994.
  - <sup>30</sup>D. N. Zheng, A. M. Campbell, J. D. Johnson, J. R. Cooper, F. J. Blunt, A. Porch, and P. A. Freeman, *Phys. Rev. B* **49**, 1417 (1994).
  - <sup>31</sup>A. Houghton, R. A. Pelcovits, and S. Sudbø, *Phys. Rev. B* **40**, 6763 (1989).
  - <sup>32</sup>S. Ali, D. N. Zheng, and D. P. Hampshire (unpublished).
  - <sup>33</sup>J. Cors, D. Cattani, M. Decroux, A. Stettler, and Ø. Fischer, *Physica B* **165-166**, 1521 (1990).
  - <sup>34</sup>N. R. Werthamer, E. Helfand, and P. C. Hohenberg, *Phys. Rev.* **147**, 295 (1966).
  - <sup>35</sup>A. A. Abrikosov, *Zh. Éksp. Teor. Fiz.* **32**, 1422 (1957) [*Sov. Phys. JETP* **5**, 1174 (1957)].
  - <sup>36</sup>J. R. Clem, *Ann. Phys. (N.Y.)* **40**, 268 (1967).
  - <sup>37</sup>B. Seeber, C. Rossel, and Ø. Fischer, in *Ternary Superconductors*, edited by G. K. Shenoy, B. D. Dunlap, and F. Y. Fradin (North-Holland, Amsterdam, 1981), p. 119.
  - <sup>38</sup>P. Birrer, F. N. Gygax, B. Hitti, E. Lippelt, A. Schenck, M. Weber, D. Cattani, J. Cors, M. Decroux, and Ø. Fischer, *Phys. Rev. B* **48**, 16 589 (1993).
  - <sup>39</sup>W. A. Fietz, M. R. Beasley, J. Silcox, and W. W. Webb, *Phys. Rev.* **136**, A335 (1964).
  - <sup>40</sup>P. W. Anderson and Y. B. Kim, *Rev. Mod. Phys.* **36**, 39 (1964).
  - <sup>41</sup>Y. Xu, M. Suenaga, A. R. Moodenbaugh, and D. O. Welch, *Phys. Rev. B* **40**, 10 882 (1989).
  - <sup>42</sup>G. Rimikis, W. Goldacker, W. Specking, and R. Flükiger, *IEEE Trans. Magn.* **27**, 1116 (1991).
  - <sup>43</sup>H. Yamasaki, M. Umeda, Y. Kimura, and S. Kosada, *IEEE Trans. Magn.* **27**, 1112 (1991).
  - <sup>44</sup>C. Rossel and Ø. Fischer, *J. Phys. F* **14**, 455 (1984).
  - <sup>45</sup>L. A. Bonney, T. C. Willis, and D. C. Larbalestier, *IEEE Trans. Appl. Supercond.* **3**, 1582 (1993).
  - <sup>46</sup>W. A. Fietz and W. W. Webb, *Phys. Rev.* **178**, 657 (1969).
  - <sup>47</sup>A. M. Campbell and J. E. Evetts, *Adv. Phys.* **21**, 199 (1972).
  - <sup>48</sup>E. J. Kramer, *J. Appl. Phys.* **44**, 1360 (1977).
  - <sup>49</sup>D. Dew-Hughes, *Philos. Mag.* **30**, 293 (1974).
  - <sup>50</sup>D. P. Hampshire and H. Jones, *J. Phys. C* **21**, 419 (1987).
  - <sup>51</sup>M. O. Rikel, T. Togonidze, and V. Tsebro, *Sov. Phys. Solid State* **28**, 1496 (1986).
  - <sup>52</sup>E. H. Brandt, *Phys. Lett.* **77A**, 484 (1980).
  - <sup>53</sup>V. R. Karasik, M. O. Rikel', T. G. Togonidze, and V. I. Tsebro, *Sov. Phys. Solid State* **27**, 1889 (1985).
  - <sup>54</sup>A. Gupta, M. Decroux, P. Selvam, D. Cattani, T. C. Willis, and Ø. Fischer, *Physica C* **234**, 219 (1994).